# Experimental Flow Studies of the Colloid Core Reactor Concept

B. N. TURMAN* AND SIEGFRIED H. HASINGER†
*Aerospace Research Laboratories (AFSC), Wright-Patterson Air Force Base, Ohio*

## Theme

NEW experiments with heavily loaded two-component vortex flows show that the interpretation of particle behavior in terms of a rotating fluidized bed model, previously established for small length/diameter ratios, is valid for length/diameter ratios approaching unity. Experimental data demonstrate that air injection on the end-wall contributes significantly to the net angular velocity of the rotating particle cloud, and that simplifying assumptions made for the tangential force balance are reasonable. The rotating fluidized bed model allows extrapolation of these experiments to the operating regime for a conceptual colloid core reactor.

## Contents

Earlier experiments[1] with particle laden vortex flows were performed with a short chamber having a length/diameter ratio of only 0.2. It was observed that solid particles in the vortex concentrated near the chamber periphery, forming an annular cloud with particle volume fraction of some 10%. Measurements of angular velocity and radial pressure drop across the cloud indicated that centrifugal force on the cloud was balanced by pressure drop, i.e., the particle suspension was in a state of fluidization. A mathematical expression for this radial force balance was obtained by extending analytical considerations for a columnar fluidized bed to the rotating case. With the inclusion of wall friction in a tangential force balance, this flow model was used to extrapolate experimental results to other flow conditions and chamber geometries. Experimental data now give support to extrapolations involving chamber geometries with length/diameter ratios approaching unity, the region of interest for colloid core reactor applications.

Figure 1 shows the basic chamber used for these experiments. The axial length of this chamber was modified by using vanes of various lengths. With a chamber diameter of 30.4 cm, axial lengths of 6.3 cm, 12.6 cm, and 18.9 cm were available. Air was injected at the chamber periphery through slots formed by the vane overlap; a series of nozzles on the end-wall, near the chamber outlet, provided air injection to the wall boundary layer. The mean diameter for talc powder used in the experiments was 18 $\mu$.

The rotating fluidized bed model of the powder loaded vortex assumes the radial thickness of the bed to be uniform in the axial direction. This assumption implies that the bed thickness is independent of chamber length for a constant powder load per unit chamber length $M/h$. The close coincidence of the density curves in Fig. 2 clearly supports this assumption. The radial density profiles of Fig. 2 were

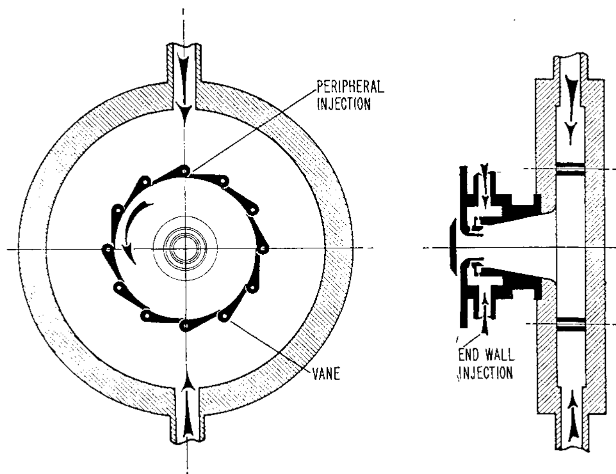


**Fig. 1 End view and side view of vortex chamber.**

obtained from X-ray absorption measurements[2] for three different chamber lengths, and constant $M/h$. Tests have also shown that the magnitude of particle loss from the vortex is essentially independent of chamber length, indicating that circulation patterns within the vortex are independent of axial length. The ratio of particle mass loss to gas flow rate in these experiments is of the order of $10^{-3}$–$10^{-4}$.

Another important finding of the present experiments is that end-wall injection, in addition to energizing the end-wall boundary layer,[1] provides a substantial input of angular momentum to the rotating particle cloud. Figure 3 shows the angular velocity of the rotating cloud plotted against the dimensionless radius of the vortex. The solid curves for total powder loads $M$ of 300 g and 700 g, are determined experimentally for an end-wall injection rate to total injection rate ratio of $\dot{m}_{ew}/\dot{m} = 0.6$. The dashed lines indicate calculated conditions for constant circulation $\Gamma$ in the cloud. As expected from conservation of angular momentum, the data

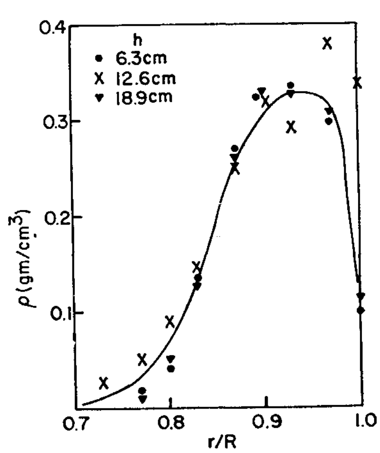


**Fig. 2 Radial distributions of particle density, for various axial chamber lengths; $M/h = 80$ g/cm.**

Presented at the 2nd Symposium on Uranium Plasmas: Research and Applications, Atlanta, Ga. November 15–17, 1971; submitted December 27, 1971; synoptic received June 7, 1972. Full paper available from AIAA Library, 750 Third Avenue, New York, N.Y. 10017. Price: Microfiche, $1.00; hard copy, $5.00.

Full paper also is included in bound volume of preprints, which is available from AIAA, 1290 Avenue of Americas, New York, N.Y. 10019. Price: $28.40.

Index categories: Nuclear Propulsion; Multiphase Flows.

* Research Physicist, Energy Conversion Research Laboratory.

† Research Scientist, Energy Conversion Research Laboratory.

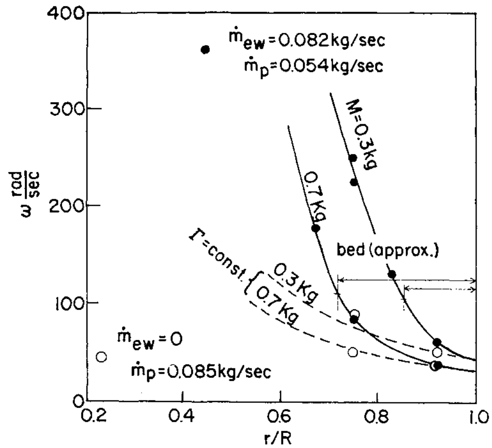


**Fig. 3 Angular velocity of vortex as function of radius, obtained from paddle wheel measurements. Approximate radial extent of the fluidized bed is sketched on graph; $\dot{m}_{ew}$ is gas flow rate through end-wall injection system, and $\dot{m}_p$ is flow rate injected at periphery.**

points for zero end-wall injection (with gas injection only at the periphery) follow approximately the constant Γ curves. The figure shows that with high percentage of end-wall injection, a strong increase of angular velocity occurs toward the inner cloud boundary, due to momentum input from end-wall injection. This finding shows that end-wall injection must be

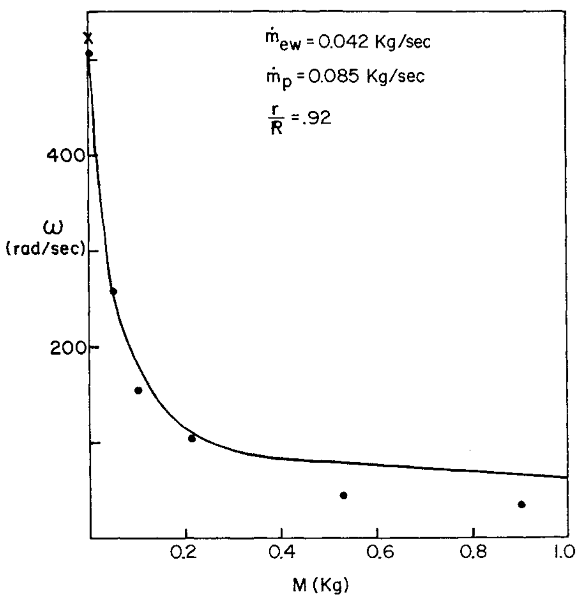


**Fig. 4 Angular velocity as function of total powder mass; solid curve is calculated from Eq. (1), and points are from paddle wheel measurements.**

**Table 1 Projected reactor parameters**

| | |
|---|---|
| Thrust | 22,000 lbf |
| Specific impulse | 1,000 lbf sec/lbm |
| Chamber radius | $R = 30$ cm |
| Chamber length | $h = 30$ cm |
| Fuel mass $(1U - 10Zr)C$ | $M = 20$ kg |
| Gas flow rate | $\dot{m} = 10$ kg/sec |
| Gas injection velocity | $v_0 = 50$ m/sec |
| Fuel volume fraction | $\eta = 0.03$ |
| Inner bed radius | $r = 13$ cm |
| Inner bed velocity | $\omega = 300$ rad/sec |
| Fluidizing pressure drop | 10 atm |

considered in the tangential force balance on the particle cloud. From the previously established flow model, the circulation at the inner cloud boundary is then

$$\Gamma = \Gamma_R/[1 + 2\pi\bar{\rho}c_f(R - r)\Gamma_R/\dot{m}] \tag{1}$$

with $\Gamma_R$ the circulation at the periphery $R$, $\bar{\rho}$ the average cloud density, $c_f$ wall friction coefficient, and $\dot{m}$ total injected mass flow rate. Figure 4 compares angular velocity calculated from this equation, using experimental values for cloud density, with velocity data obtained from paddle wheel measurements. Agreement appears reasonably good, particularly at low total mass load.

These experiments indicate that the rotating fluidized bed model is valid over a wide range of vortex chamber length/diameter ratios, and no adverse particle containment problems arise as length/diameter ratio approaches unity. These observations are particularly important for the colloid core reactor concept, because a larger length/diameter ratio geometry is more favorable from a nucleonics viewpoint. Some projected values for operating conditions of such a reactor, as derived from the fluidized bed model, are listed in Table 1. The powder mass shown in the table is based on critical mass calculations of Tang et al.[3] That nuclear analysis was limited to length/diameter ratio less than 0.2: the possibility now is open for optimization of the chamber geometry to accommodate both the nucleonic and aeromechanical requirements.

## References


[1] Anderson, L. A., Hasinger, S. H., and Turman, B. N., "Two-Component Vortex Flow Studies of the Colloid Core Nuclear Rocket," *Journal of Spacecraft and Rockets*, Vol. 9, No. 5, May 1972, pp. 311–317.

[2] Turman, B. N. and Perrault, R. E., "Application of Radiographic Techniques to Studies of Particle Laden Flow," Rept. 72-0007, 1972, Aerospace Research Lab., Wright-Patterson Air Force Base, Ohio.

[3] Tang, Y. S., Stefanko, J. S., Dickson, P. W., and Drawbaugh, D. W., "An Engineering Study of the Colloid-Fueled Reactor Concept," *Journal of Spacecraft and Rockets*, Vol. 8, No. 2, Feb. 1971, pp. 129–133.